ELSEVIER

Journal of Organometallic Chemistry 575 (1999) 171–181

Journal of Organometallic Chemistry

Ruthenocenyl ruthenium bimetallic complexes: electrospray mass spectrometric study of $[RuX(\eta^5\text{-}C_5H_5)(\eta^2\text{-dppr})]^{n+}$ (dppr = 1,1′-bis(diphenylphosphino)ruthenocene) (X = Cl, $n = 0$; X = CO, CH_3CN, C≡CHPh, $n = 1$) and the X-ray crystal and molecular structure of $[Ru(\eta^5\text{-}C_5H_5)(CO)(\eta^2\text{-dppr})]PF_6$

Siew Po Yeo [a], William Henderson [b], Thomas C.W. Mak [c], T.S. Andy Hor [a,*]

[a] *Department of Chemistry, Faculty of Science, National University of Singapore, Kent Ridge, 119260 Singapore, Singapore*
[b] *Department of Chemistry, University of Waikato, Private Bag 3105, Hamilton, New Zealand*
[c] *Department of Chemistry, The Chinese University of Hong Kong, Shatin, NT, Hong Kong*

Received 15 July 1998; received in revised form 19 September 1998

Abstract

$[RuCl(Cp)(PPh_3)_2]$ ($Cp = \eta^5\text{-}C_5H_5$) reacts with dppr in refluxing benzene to give [RuCl(Cp)(dppr)], **1**, {dppr = $[Ru(\eta^5\text{-}C_5H_4PPh_2)_2]$} in 91% yield. Complex **1** ionizes in boiling acetonitrile in the presence of excess NH_4PF_6 to give $[Ru(Cp)(CH_3CN)(dppr)]PF_6$, **2**, in 76% yield. Under CO at 60°C, **1** converts to [Ru(Cp)(CO)(dppr)]Cl, **3a**, whose derivative $[Ru(Cp)(CO)(dppr)]PF_6$, **3b**, can also be obtained from **2** in 86% with CO. With HC≡CPh, **2** instantaneously gives a vinylidene complex, $[Ru(C{=}CHPh)(Cp)(dppr)]PF_6$, **4**, quantitatively (98%). The kinetic stability of the η^2-coordinated dppr ring is evident in these reactions. The X-ray molecular structure of **3b** [space group $P2_1/c$, $a = 9.990(2)$, $b = 19.498(4)$, $c = 19.113(4)$ Å and $\beta = 96.21(3)°$] reveals a pseudo-octahedral Ru(II) structure with a η^5-Cp, a chelated dppr, a terminal CO and an uncoordinated PF_6^- anion. It is the first piano-stool dppr structure characterized by X-ray single-crystal diffractometry. The dppr chelate has a large bite (100.5(1)°) and there is no direct interaction between the two Ru(II) centers (Ru(1)···Ru(2) 4.389 Å). The electrospray mass spectra (ESMS) of **2**–**4** generally give peaks due to the intact cations at low cone voltages. As the cone voltage increases, fragmentation commences which inevitably gives $[Ru(Cp)(dppr)]^+$ as the primary fragment ion. In-situ doping of dppr with $AgNO_3$ gives $[Ag(dppr)]^+$ as the major species plus $[Ag(dppr)_2]^+$ (m/z 1307) and other oxidized by-products. Similar treatment of **4** gives an acetylide complex $[Ag\{Ru(Cp)(C{\equiv}CPh)(dppr)\}_2]^+$ (m/z 1843) at 20 V which ejects one Ru metalloligand to give $[Ag\{Ru(Cp)(C{\equiv}CPh)(dppr)\}]^+$ (m/z 975) at higher voltages. Complex **4** is hydrogenated with H_2 gas to give ethylbenzene in 55% yield after 4 h in refluxing THF. It also catalyzes the hydrogenation of HC≡CPh to give 52% of ethylbenzene in 5 h at 5 mol.% catalyst level.

Keywords: Ruthenium; Metallocenyl phosphine; Vinylidene; Electrospray mass spectrometry; Crystal structure

1. Introduction

Many organic reactions, notably cross-coupling, Grignard-type couplings, Heck reactions, hydroformylations and hydrogenations, are catalyzed by metal phosphine complexes [1]. The phosphines used include both monophosphines and diphosphines. In some cases, the chelate effect of the latter appears to promote the catalytic efficiency. When the diphosphine is metallocene-based such as 1,1′-bis(diphenylphosphino)-ferrocene (dppf), such catalytic enhancement is further manifested [2]. Even though in many cases understanding of the role played by the diphosphine

* Corresponding author. Tel.: +65-8742917; fax: +65-7774279; e-mail: chmandyh@nus.edu.sg.

0022-328X/99/$ - see front matter
PII: S0022-328X(98)00990-5

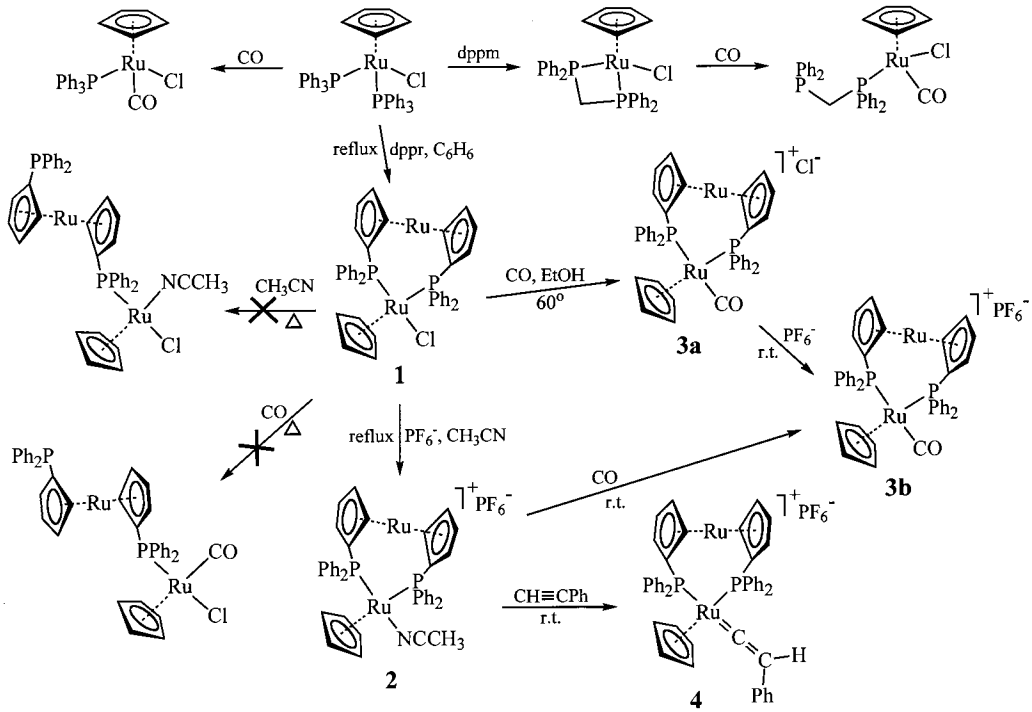

Scheme 1. Synthesis of [RuCl(Cp)(dppr)], **1**, and its substitution reactions with CO, CH_3CN and HC≡CPh.

and even the catalytic mechanism in general is very tentative, it does not deter the use of these metallocenyl diphosphines as ligands in catalytic systems. The common use of dppf today is such an example [3]. Although many of the advantages of dppf can in principle be manifested in its ruthenocene analogue, viz. 1,1′-bis (diphenylphosphino)ruthenocene (dppr), due to its larger ring separation and bigger chelate bite, the use of dppr complexes is still at its infancy. This problem is partly attributed to the lack of established dppr complexes in the literature. Recently, we reported the synthesis and catalytic behavior of $[MCl_2(dppr)]$ (M = Ni, Pd and Pt) [4] and the chemistry of $[RuCl_2(dppr)(L)]$ ($L = PPh_3$, CO, CH_3CN) [5]. We herein extend our investigations to the synthesis of [RuCl(Cp)(dppr)] and its reactivity towards some representative small molecules such as CO, CH_3CN and HC≡CPh. Many of the complexes isolated are studied by electrospray (ionization) mass spectrometry (ESMS) [6], which is rapidly gaining recognition as a versatile mass spectrometry with a soft ionization process. It is particularly useful for the characterization of organometallic complexes in solution [7]. The fragmentation patterns at different cone voltages can often yield invaluable structural insight on the complexes [8]. In this paper, we report the use of ESMS, assisted by other techniques, in the study of a series of bimetallic ruthenium ruthenocenyl phosphine complexes. We also report the use of $AgNO_3$ as a doping technique for the ESMS identification of other species that have not yet been isolated. The catalytic potential of the Ru–dppr system is also explored. The reactions described are compared with those of [RuClCp(L)] ($L = 2 \times PPh_3$, dppm, dppe and dppf [dppm = bis(diphenylphosphino)methane; dppe = 1,2-bis(diphenylphosphino)ethane]) [9]. Our interest in the Ru(II) system stems from its potential shown in catalysis especially in chiral synthesis [10] and hydrogenation [11], for example, Ru(II) diphosphine (binap) (binap = 2,2′-bis(diphenylphosphino)-1,1′-binaphthyl) complexes in Naproxen® synthesis [12].

2. Results and discussion

Phosphine replacement in $[RuCl(Cp)(PPh_3)_2]$ with dppr occurs readily in refluxing benzene to give [RuCl(Cp)(dppr)], **1** in 91% yield. Complex **1** ionizes in boiling CH_3CN in the presence of excess NH_4PF_6 to give the acetonitrile complex $[Ru(Cp)(CH_3CN)(dppr)]PF_6$, **2** in 76% yield. Chloride displacement of **1** by CO giving [Ru(Cp)(CO)(dppr)]Cl, **3a**, occurs at 60°C in EtOH under an atmospheric pressure of CO gas. Formation of the PF_6^- derivative of **3**, viz. **3b**, can be effected at room temperature (r.t.) and with high yield (86%) when **2** is used as the substrate. The advantage in using a labile solvent complex in ligand substitution reactions is also evident when **2** absorbs HC≡CPh rapidly (within seconds) at r.t. to give $[Ru(C{=}CHPh)(Cp)(dppr)]PF_6$, **4** in near-quantitative (98%) yield. These reactions are summarized in Scheme 1.

Formation of **1** from $[RuCl(Cp)(PPh_3)_2]$ represents a facile substitution of PPh_3 by dppr. This is somewhat surprising considering that a bulky ligand such as dppr is not expected to gain much entropy advantage on the chelate effect and that a number of dppr complexes are known to be kinetically labile [13]. The stability of the η^2-coordinated dppr is possibly attributed to the better π-accepting ability of dppr as a result of the conjugation of the π^* orbitals of C_5 rings with the empty d-orbitals of the phosphorus atoms. The higher acidity of dppr is expected to contract the 4d orbitals of Ru which could then overlap better with the filled 3p-orbitals of Cl. This proposed strengthening of the Ru–Cl interaction receives some experimental support as **1** is insoluble in MeOH in which its PPh_3 analogue [14] readily dissolves by ionization. All the PPh_3, PMe_3 [15], dppm ([9]a) and dppe ([9]a) derivatives ionize easily in acetonitrile through chloride dissociation whereas for **1**, the assistance from NH_4PF_6 is needed in its chloride extraction to give **2**. There is no evidence that a ring opening reaction giving $[RuCl(Cp)(CH_3CN)(\eta^1\text{-dppr})]$ would proceed. The integrity of the chelate ring is maintained even under reflux conditions in a donor solvent such as CH_3CN. The carbonylation of **1** giving **3** reiterates the stability of the bimetallic chelate and the ability for **1** to accept a 2-electron donor. This absorption of CO is sluggish at r.t. but proceeds readily at 60°C. However, the labile CH_3CN ligand in **2** exchanges with CO readily at r.t. The ^{31}P-NMR resonance of **3** is more deshielded compared to **1** or **2**. This is consistent with the incorporation of a strongly π-acidic CO. Again, there is no evidence for the formation of $[RuCl(Cp)(CO)(\eta^1\text{-dppr})]$. This is in sharp contrast to the analogous reactions of the PPh_3 and dppm derivatives which give $[RuCl(Cp)(CO)(PPh_3)]$ [14] and $[RuCl(Cp)(CO)(\eta^1\text{-dppm})]$ ([9]a), respectively (see Scheme 1). These differences support the kinetic stability of the ring and demonstrate the different behaviors between dppr and other phosphines. Similar work on the reaction of CO with $[RuCl_2(dppr)(PPh_3)]$ also reports a PPh_3 substitution to give $[RuCl_2(CO)(dppr)]$ rather than chloride displacement or ring opening of the chelating phosphine [5].

Among the few dppr complexes reported in the literature, the only one which was crystallographically characterized was $[PtCl_2(dppr)]$ [4]. We intended to study the X-ray structure of **3b** and establish the bimetallic chelate ring characteristics of dppr in an expected piano-stool environment in **3**. The X-ray molecular structure of **3b** confirms such a structure with a tetrahedral ruthenium bearing a η^5-Cp, a dppr chelate and a terminal CO with an uncoordinated PF_6^- anion (see Fig. 1 and Tables 1–3). The dppr chelate forms a closed loop with the central ruthenium with no direct interactions between the two Ru(II) centers (Ru(1)···Ru(2) 4.389 Å). This loop can be viewed as a

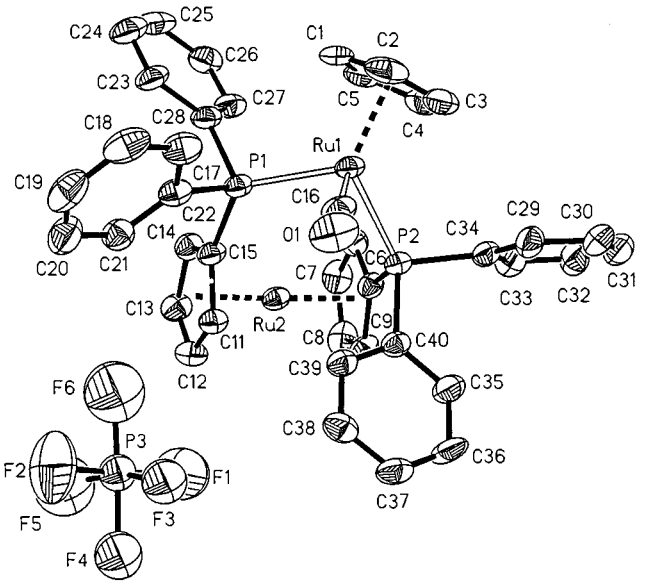

Fig. 1. An ORTEP drawing of the molecular structure of $[Ru(Cp)(CO)(dppr)]PF_6$, **3b**, (35% thermal ellipsoids)

rhombus with the Ru atoms occupying two opposite corners and the P atoms sitting at the remaining two. The significantly different steric requirements of dppr and CO forces some distortions among the legs of the stool (C(16)–Ru(1)–P(1) 92.3(3)°, C(16)–Ru(1)–P(2) 91.6(3)° and P(1)–Ru(1)–P(2) 100.5(1)°). The chelate angle (100.5(1)°) is larger than those reported in the piano-stool M–dppf structures ([(Ru(Cp)H(dppf)] ([9]b) 95.5(1) and 99.1(1)°; [Mn(MeCp)(CO)(dppf)] [16] 99.3(12)°). Such a large chelate bite however does not destabilize the metal chelate ring. In agreement with the

Table 1
Crystallographic data and refinement details for $[Ru(\eta^5\text{-}C_5H_5)(CO)(dppr)][PF_6]$ **3b**

Chemical formula	$C_{40}H_{33}OF_6P_3Ru_2$
M	938.7
Crystal system	Monoclinic
Space group	$P2_1/c$
a (Å)	9.990(2)
b (Å)	19.498(4)
c (Å)	19.113(4)
β (°)	96.21(3)
V (Å^3)	3701(2)
Z	4
$F(000)$	1872
$D_{calc.}$ (g cm^{-3})	1.685
μ (mm^{-1})	1.01
Mean μr	0.09
Transmission factors	0.574–1.000
R_F[a]	0.055
R_w[b]	0.075
S[c]	1.13

[a] $R_F = \Sigma\|\|F_o\|-|F_c\|\|/\Sigma|F_o|$.
[b] $R_w = [\Sigma w(|F_o|-|F_c|)^2/\Sigma w|F_o|^2]^{0.5}$.
[c] S (goodness-of-fit) $= [\Sigma w(|F_o-|F_c|)^2/(n-p)]^{0.5}$.

Table 2
Selected bond lengths (Å) for [Ru(η^5-C_5H_5)(CO)(dppr)][PF_6] **3b**

Atoms	Length (Å)	Atoms	Length (Å)
Ru(1)–C(16)	1.84(1)	Ru(1)–P(1)	2.361(3)
Ru(1)–P(2)	2.351(2)	Ru(1)–X(1A)[a]	1.897(8)
Ru(2)–X(1B)	1.799(9)	Ru(2)–X(1C)	1.804(9)
C(16)–O(1)	1.16(1)	C(1)–C(2)	1.41(2)
C(1)–C(5)	1.39(2)	C(2)–C(3)	1.39(2)
C(3)–C(4)	1.42(2)	C(4)–C(5)	1.37(2)
C(6)–C(7)	1.41(2)	C(6)–C(10)	1.43(1)
C(7)–C(8)	1.39(2)	C(8)–C(9)	1.41(2)
C(9)–C(10)	1.44(1)	C(10)–P(2)	1.823(9)
C(11)–C(12)	1.39(1)	C(11)–C(15)	1.41(1)
C(12)–C(13)	1.40(1)	C(13)–C(14)	1.43(1)
C(14)–C(15)	1.40(1)	C(15)–P(1)	1.845(9)

[a] X(1A), X(1B) and X(1C) represent centroids of the rings of (C1, C2, C3, C4, C5), (C6, C7, C8, C9, C10) and (C11, C12, C13, C14, C15), respectively.

NMR data that support dppr as a good π-acid character, the Ru–P bonds strengthen from 2.43 Å in [RuCl(Cp)(PPh_3)$_2$] [15] to 2.356(3) Å in **3b**. The competition for π electrons weakens the Ru–Cp bonds from 1.846(6) Å in [RuCl(Cp)(PPh_3)$_2$] to 1.897(8) Å in **3b**. The terminal CO is slightly bent (Ru(1)–C(16)–O(1) 173.3(8)°) in order to avoid extending into the ruthenocenyl region. Coordination of dppr expectedly weakens the phosphorus link to the C_5 ring from 1.808(4) Å in the free ligand [4] to an average of 1.834(9) Å in **3b**. The substitutionally-induced C–C bond variations among the C_5 rings are less obvious in **3b** (C_p–C_α 1.42(1), C_α–C_β 1.41(2), C_β–C_γ 1.40(2) Å) than in the free ligand (1.432(5), 1.413(6), and 1.402(6) Å, respectively). The coordination of the dppr ligand imposes some differences between the two C_5 rings and their PPh_2 residues.

Table 3
Selected bond angles (°) for [Ru(η^5-C_5H_5)(CO)(dppr)][PF_6] **3b**

Atoms	Angle (°)	Atoms	Angle (°)
C(16)–Ru(1)–X(1A)[a]	121.6(5)	C(16)–Ru(1)–P(1)	92.3(3)
C(16)–Ru(1)–P(2)	91.6(3)	P(1)–Ru(1)–X(1A)	121.0(3)
P(2)–Ru(1)–X(1A)	122.1(4)	P(1)–Ru(1)–P(2)	100.5(1)
Ru(1)–C(16)–O(1)	173.3(8)	X(1B)–Ru(2)–X(1C)	177.4(4)
C(15)–P(1)–C(28)	99.1(4)	C(15)–P(1)–C(22)	101.0(4)
C(22)–P(1)–C(28)	102.2(4)	C(10)–P(2)–C(34)	102.7(4)
C(10)–P(2)–C(40)	103.6(4)	C(40)–P(2)–C(34)	100.2(4)
Ru(1)–P(1)–C(15)	125.2(3)	Ru(1)–P(1)–C(22)	113.7(3)
Ru(1)–P(1)–C(28)	112.5(3)	Ru(1)–P(2)–C(10)	117.8(3)
Ru(1)–P(2)–C(34)	112.4(3)	Ru(1)–P(2)–C(40)	117.7(3)

[a] X(1A), X(1B) and X(1C) represent centroids of the rings of (C1, C2, C3, C4, C5), (C6, C7, C8, C9, C10) and (C11, C12, C13, C14, C15), respectively.

To accommodate the large bite angle, both C_5 rings are tilted inwards towards Ru(1). This causes a slight distortion from linearity on the angle subtended by Ru(2) to the two centroids of the C_5 rings (177.4(4)°). The large chelate bite could force stronger interactions among the co-ligands. It also helps to stabilize the unsaturated complex upon departure of the third ligand, Cl, CO or CH_3CN. With these in mind, the catalytic study of the hydrogenation of HC≡CPh with **4** becomes meaningful.

The rapid formation of **4** from **2** demonstrates the ability of the latter to activate unsaturated organic substrates at r.t. The identification of a vinylidene complex as opposed to a π-bonded alkyne complex [Ru(Cp)(HC≡CPh)(dppr)]PF_6 or σ-bonded acetylide complex [Ru(Cp)(C≡CPh)(dppr)] is based on the IR[1] and NMR data and the related PPh_3 and dppf complexes [17]. Weak coupling between the vinylic proton and phosphorus [^4J(P–H) 1.9 Hz] is observed. Conclusive evidence comes from the exceedingly low field shift of the C_α atom (carbon bonded to Ru) (354.0 ppm), which has been explained based on the paramagnetic contribution of nuclear shielding [18]. Similar η^2-alkyne complexes would give ^{13}C shifts which are at significantly higher field ($\sim$50 ppm) [19]. It is interesting to note that a similar addition of HC≡CPh to [RuCl(Cp*)(P–P)] (P–P = diop (diop = {[(2,2-dimethyl-1,3-dioxolan-4,5-diyl)bis(methylene)]bis(diphenylphosphine)}) or binap) in the presence of NH_4PF_6 and Al_2O_3 gives an acetylide complex [20] whereas many of the others, including **4**, result in vinylidene complexes. Formation of **4** from **2** likely takes place by an established mechanism which involves ethyne addition, followed by a slippage with a concerted 1,2-hydrogen shift [21]. An alternative pathway involving oxidative addition giving rise to a hydride acetylide intermediate [22] is more feasible only for metals such as Co(I) [23] and Rh(I) [24]. The significance of similar vinylidene complexes in a reconstitutive condensation of allylic alcohols and terminal alkynes has been described elsewhere [25].

Metallocenes that have been previously studied by ESMS display two ionization pathways, namely oxidation and protonation. The former route depends on the redox potential of the metallocene whereas the latter is promoted by the presence of basic substituents. In many cases, both pathways can be observed. Although

[1] The presence of two ν(C=C) bands both in the solid KBr mull and solution could suggest the presence of two isomers. For related compounds with similar IR observations, see: (a) R.M. Bullock, J. Chem. Soc. Chem. Commun. (1989) 165. (b) M.I. Bruce, F.S. Wong, B.W. Skelton, A.H. White, J. Chem. Soc. Dalton Trans. (1982) 2203. For isomers of vinylidene complexes, see: (c) Y. Wakatsuki, N. Koga, H. Yamazaki, K. Morokuma, J. Am. Chem. Soc. 116 (1994) 8105.

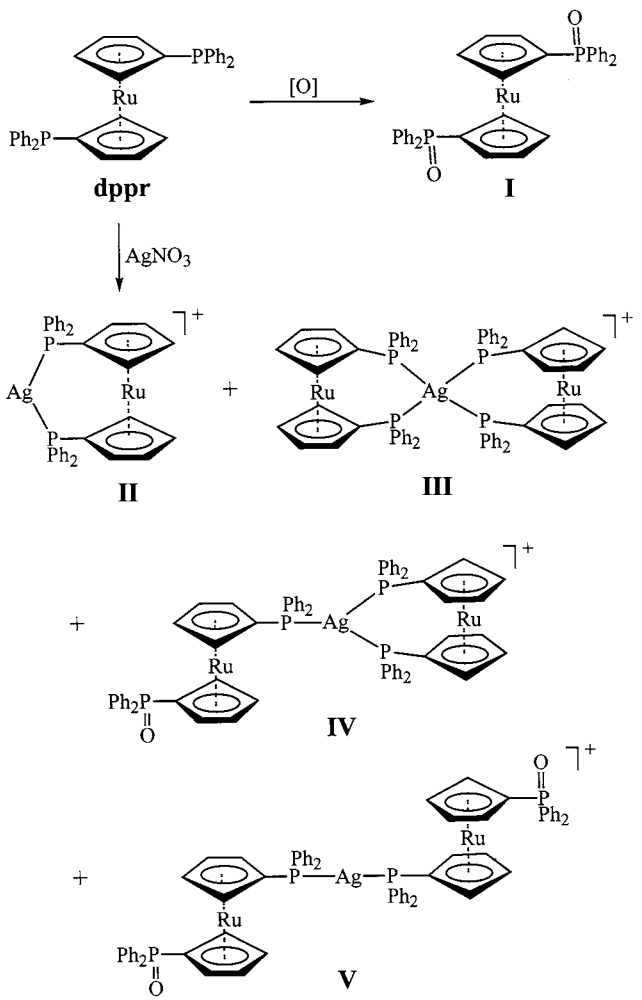

Scheme 2. ESMS fragmentation pattern of dppr and its addition to $AgNO_3$.

dppr in CH_3CN does not show any peak corresponding to the parent ion $[dppr]^+$, its oxidation product, $\{Ru[(\eta^5\text{-}C_5H_4)P(O)Ph_2]_2\}$ ($dpprO_2$), (**I**), (m/z 632) is detected as its $[M+H]^+$ ion. Doping with a drop of $AgNO_3$ to the analyte solution gives $[Ag(dppr)]^+$ (**II**) (m/z 709) as the major species and $[Ag(dppr)_2]^+$ (**III**) (m/z 1307) and other oxidized products such as $[Ag(dppr)(dpprO)]^+$ (**IV**) (m/z 1323) and $[Ag(dpprO)_2]^+$ (**V**) (m/z 1339) and proposed structures are given in Scheme 2. Formation of these species illustrates the ability for Ag^+ to give linear, trigonal planar and tetrahedral phosphine complexes with dppr and dpprO. In the latter case, the ligand is most likely P-bonded due to the soft character of Ag(I). A similar finding was reported in a recent study of dppf with Ag^+ by ESMS [26].

The spectrum of **2** in a CH_3CN/H_2O solution at a low cone voltage (5 V) (Fig. 2) gives the parent ion $[Ru(Cp)(CH_3CN)(dppr)]^+$ (**VI**). Upon increasing to 20 V, fragmentation begins to occur by which the CH_3CN ligand is lost to give $[Ru(Cp)(dppr)]^+$ (**VII**). Such fragmentation is almost complete at 40 V (Fig. 2 and Scheme 3). These studies suggest that the most labile ligand is ejected at the lowest voltage whilst the stronger ones would depart as the cone voltage increases. These spectra confirm the solution results in suggesting that CH_3CN is preferentially dissociated over dppr. Similar behavior is seen for $[RuCl(Cp)(PPh_3)_2]$ which gives $[Ru(Cp)(CH_3CN)(PPh_3)_2]^+$ (**IX**) (m/z 732) at low cone voltages. The acetonitrile ligand is lost to give $[Ru(Cp)(PPh_3)_2]^+$ (**X**) (m/z 691) when the voltage is increased to 40 V. The observed isotope patterns compare well with the calculated ones. The spectra of the carbonyl complex **3** lead to a similar conclusion in that the molecular ion (**VIII**) is observed at low cone voltages. However, there is no evidence for decarbonylation when the voltage is raised to 40 V. Only when the voltage is further increased to 60 V does $[Ru(Cp)(dppr)]^+$ (**VII**) begin to appear. This is consistent with our earlier deduction that CO binds much stronger to Ru(II) than CH_3CN. Although an alternative pathway involving cyclometalation is seen in other PPh_3 complexes [27], no such phenomenon is observed for **3**. The most likely explanation is that cyclometalation of a chelated ligand would experience greater difficulty. The fragmentation pathways of **1**, **2** and **3** are summarized in Scheme 3.

The positive-ion ESMS spectrum of **4** at 20 V (Fig. 3a) shows the parent ion $[Ru(=C=CHPh)(Cp)(dppr)]^+$ (**XI**) as the main species at m/z 867. The negative-ion spectrum at 20 V also shows a single intense ion at m/z 146 for the PF_6^- counter-ion. These support the Ru–vinylidene formulation. A weak peak at m/z 433 is identified as the doubly charged molecular cation $[Ru(=C=CHPh)(Cp)(dppr)]^{2+}$ (**XII**) formed by the oxidation of the sandwiched ruthenium (Scheme 4). Such oxidation gives two different oxidation states (II, III) for both Ru centers and opens an opportunity for the study of their cooperative effects by tuning their electronic states. A weak ion at m/z 793 is tentatively assigned as the parent vinylidene species $[Ru(Cp)(C=CH_2)(dppr)]^+$. On increasing the cone voltage to 50 V (Fig. 3b), fragmentation occurs, resulting in loss of the vinylidene ligand to give $[Ru(Cp)(dppr)]^+$ at m/z 766.

Addition of a trace amount of $AgNO_3$ to a solution of **4** surprisingly gives $[Ag\{Ru(Cp)(C\equiv CPh)(dppr)\}_2]^+$ (**XIII**) as a small peak at m/z 1842 at 20 V. (Fig. 3c) This is possibly an $[AgRu_2]^+$ complex bridged by two acetylide ligands σ-bonded to Ru(II) and π-bonded to Ag(I). A similar $[AgW_2]^+$ complex has recently been observed in the ESMS of a W_2 tetrayne complex [28]. This follows an earlier work in the use of Ag^+ as an agent to promote ionization and hence spectral detection [29]. Although this $[AgRu_2]^+$ complex has not been isolated in solution, it is nevertheless significant that such acetylide-bridged complex can be detected

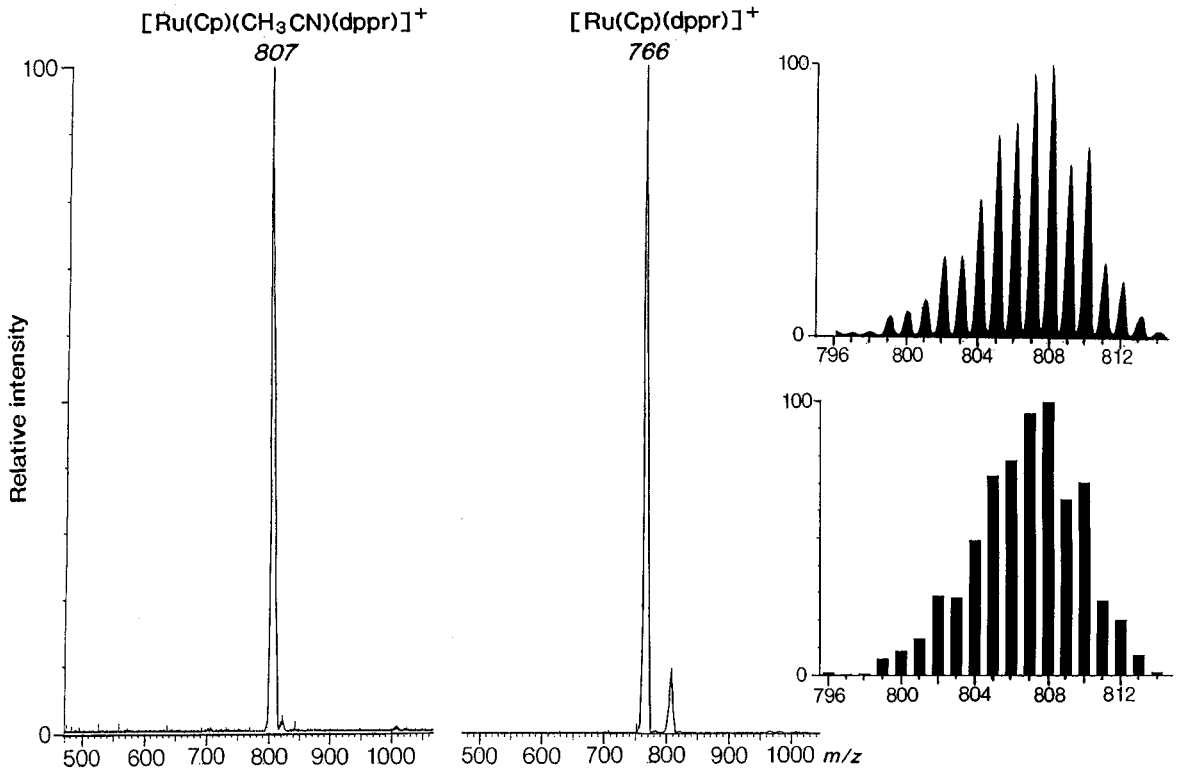

Fig. 2. Positive-ion ESMS spectra ($CH_3CN–H_2O$ solvent) of the complex $[Ru(Cp)(CH_3CN)(dppr)]PF_6$, **2** recorded at cone voltages of 5 V (left) and 40 V (right), showing the relatively facile loss of the CH_3CN ligand. The insets show the experimental (upper) and calculated (lower) isotope patterns for the parent ion $[Ru(Cp)(CH_3CN)(dppr)]^+$. The cation of the related carbonyl complex **3b** showed similar behavior, although the CO ligand did not begin to be lost until a cone voltage of 60 V.

under the ESMS conditions. Loss of the acetylide ligand from $[Ag\{Ru(Cp)(C{\equiv}CPh)(dppr)\}_2]^+$ (**XIII**) occurs at a higher cone voltage (50 V) although **XIII** is still observed. Under these conditions, a major species, $[Ag\{Ru(Cp)(C{\equiv}CPh)(dppr)\}]^+$ (**XIV**) (*m*/*z* 975) is formed, which can be explained by the cleavage of one metalloligand from **XIII**, together with $[Ru(Cp)(dppr)]^+$ (**VII**). Generation of the latter fragment is also inferred from the thermal degradation profile of **3b**. Thermogravimetric analysis (TGA) of **3b** gives a weight loss of 5.9% in the region of 50–150°C. This corresponds to the loss of solvent of crystallization and the CO ligand and gives $[Ru(Cp)(dppr)]^+$. Heating beyond 170°C would cause further decomposition to give RuO_2.

Complex **4** readily yields ethylbenzene (55%) when it is refluxed (for 4 h) in THF under an atmospheric pressure of H_2 gas. There is no evidence for the formation of styrene. This reaction becomes catalytic when a THF solution of $HC{\equiv}CPh$ is refluxed under H_2 in the presence of 5 mol% of **4**. It gives a 52% yield of ethylbenzene after 5 h. The catalytic mechanism is presently being investigated.

The kinetic stability of the ruthenocenyl ruthenium chelate ring is unexpected. It enables the development of some new chemistry parallel to but different from those of the known phosphines and diphosphines. We are especially interested in the activation of unsaturated inorganic and organic molecules and their catalytic implications. The mechanistic significance of the formation of a vinylidene complex from a terminal acetylene has been elegantly described by Caulton et al. [30]. Although our vinylidene complex (**4**) cannot be formed from the proposed Ru–H insertion into the acetylene (since our substrates are not hydrides and there is no obvious hydride source), the mechanism proposed by Caulton et al. may have some implications in the catalytic and stoichiometric hydrogenation capability shown by **4**. Research work in this direction is currently in progress.

3. Experimental section

3.1. General comments

All reactions were routinely carried out under pure dry argon using standard Schlenk techniques [31]. All solvents for the reactions were vacuum degassed before use. The solvents were of reagent grade and were freshly purified and dried by published procedures [32]. Chemical reagents, unless otherwise stated, were com-

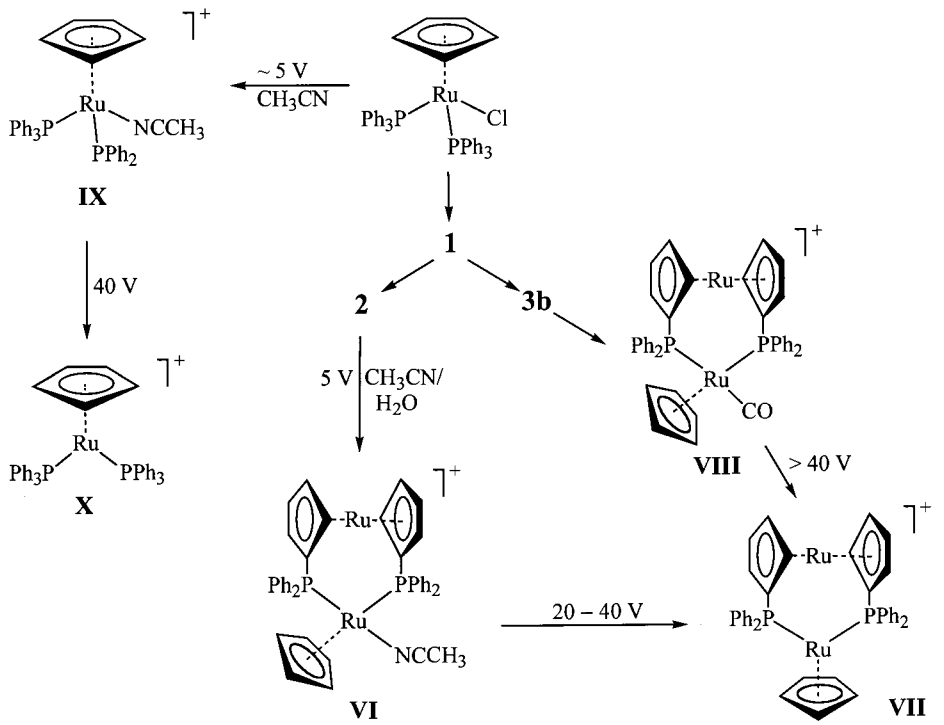

Scheme 3. ESMS fragmentation pattern of $[RuCl(Cp)(PPh_3)_2]$, [RuCl(Cp)(dppr)], **1**, $[Ru(Cp)(CH_3CN)(dppr)]PF_6$, **2** and $[Ru(Cp)(CO)(dppr)]PF_6$, **3b**.

mercial products and were used without further purification.

Room temperature one-dimensional ^{1}H-NMR spectra were recorded on either a JEOL FX 90Q Fourier transformation NMR spectrometer or a Bruker AC 300F spectrometer, at 89.55 or 299.96 MHz, respectively, with $(CH_3)_4Si$ as internal standard. ^{31}P-NMR spectra were also recorded on these instruments at 36.23 or 121.49 MHz, respectively. The phosphorus chemical shifts were quoted from the proton-decoupled spectra, and are reported in ppm to the higher frequency of external 85% H_3PO_4. ^{13}C-NMR spectra were recorded only on a Bruker AC 300F spectrometer. The carbon chemical shifts were quoted from the proton-decoupled spectra, with $(CH_3)_4Si$ as internal standard. Air sensitive samples were prepared inside a Schlenk tube under argon.

Fourier transform IR spectra were recorded with either a Perkin-Elmer 1725X or a Bio-rad FTS-165 FT-IR spectrometer. All spectra were recorded at r.t. either in the solution or solid phase. For the solution phase IR, liquid cells with NaCl windows were used. The cells were equipped with PTFE spacers giving a pathlength of 0.1 mm. Air-sensitive solutions were introduced into the cell via a syringe after the cell was flushed with argon gas. The openings of the cell were then sealed with 5 mm red rubber septa. Solid phase IR spectra were recorded in samples pulverized with KBr.

Elemental analyses were conducted at the Microanalytical Laboratory, Department of Chemistry, National University of Singapore. Some data of selected compounds are unsatisfactory despite repeated purification and analysis. We attribute this to problems faced in the acid digestion of these bimetallic compounds. The identification and purity of these compounds are supported by spectroscopy (NMR) and thermal analyses (TG & DSC). Thermogravimetry (TG) and derivative thermogravimetry analysis (DTG) were conducted using the DuPont Instruments 910 DSC and 951 TGA. All catalytic results were analyzed by gas chromatography (Hewlett-Packard 5890 series II) using a HP/I/cross-linked methyl silicone gum column (25 m × 0.32 mm × 0.52 μm film thickness). Results were plotted by the HP 3396 Series II integrator. Analysis was performed by injecting 1.0 μl of a sample of filtered reaction mixture into the gas chromatogram. The initial temperature of 30°C was maintained for 1 min, thereafter increasing at a rate of 10°C min^{-1} before reaching the maximum temperature of 180°C and holding it for another minute. Standards of phenylacetylene, styrene, ethylbenzene, toluene and THF were checked for their retention times. Toluene was used as the internal standard for the calibration of standards. Calibration using mixtures of toluene and ethylbenzene were carried out.

3.2. Synthesis of [1,1′-bis(diphenylphosphino)-ruthenocene]chlorocyclopentadienyl-ruthenium(II) [$RuCl(\eta^5\text{-}C_5H_5)(dppr)$] (**1**) from dppr

A solution of [$RuCl(\eta^5\text{-}C_5H_5)(PPh_3)$] (0.140 g, 0.193 mmol) and dppr (0.17 g, 0.284 mmol) in benzene (25 ml) was refluxed for 16 h. The solution was evaporated to dryness under reduced pressure and this crude product was suspended in CH_2Cl_2 (5 ml) to which absolute alcohol (15 ml) was added with rapid stirring. The supernatant liquid was removed using a syringe. This process of suspension, alcohol addition and solvent removal was repeated. The residue was recrystallized in CH_2Cl_2–hexane (1:3) to give yellow–orange crystals of $\mathbf{1}\cdot 0.5C_6H_{14}$. Yield: 0.14 g, 91%. The same product was obtained when a two molar excess of dppr was used. Anal. Calc. for $C_{42}H_{40}P_2ClRu_2$: C, 59.7; H, 4.8; P, 7.3; Cl, 4.2; Ru, 23.9%. Found: C, 59.2; H, 4.2; P, 7.8; Cl, 5.5; Ru, 22.0%. δ_H ($CDCl_3$): 3.97 (s, Cp, 5H); 4.44 (m, C_5H_4, 2H); 4.65 (m, C_5H_4, 2H); 4.80 (m, C_5H_4, 2H); 5.46 (m, C_5H_4, 2H); 7.26 – 7.87 (m, C_6H_5, 20H) ppm. δ_P: 42.2 (s) ppm.

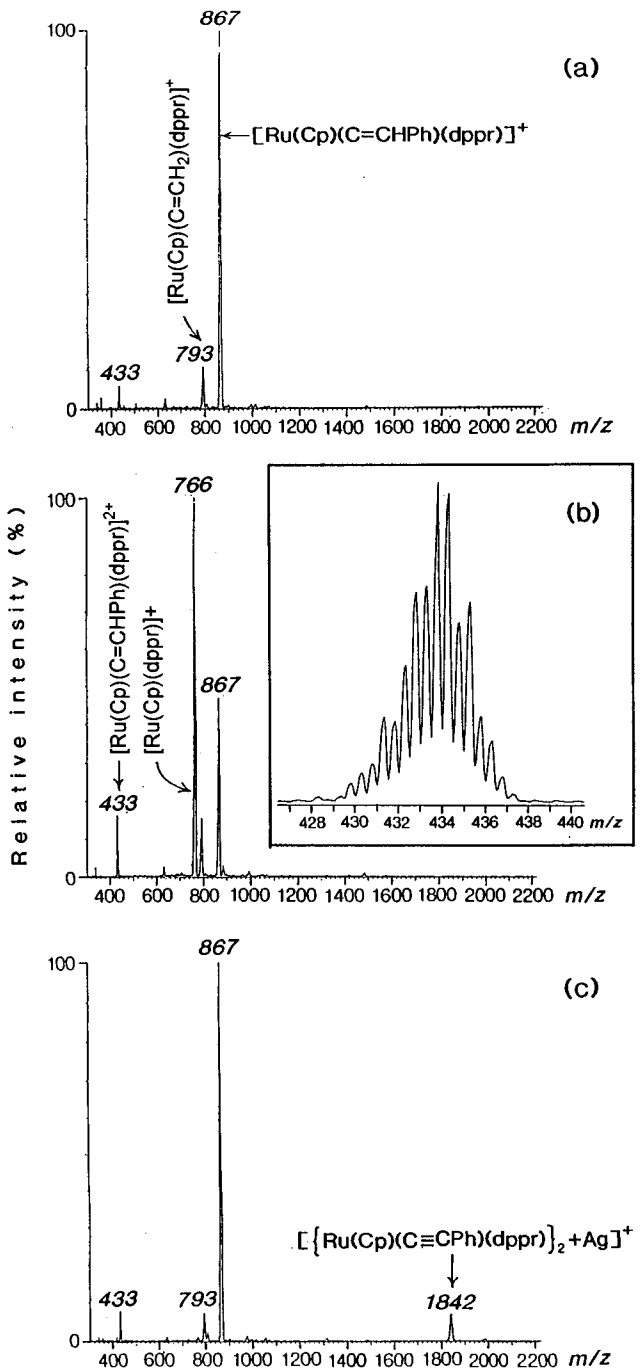

Fig. 3. Positive-ion ESMS spectrum of complex **4** recorded in methanol solution at cone voltages of (a) 20, (b) 50 , and (c) 20 V after the addition of $AgNO_3$. Inset to (b): this shows the isotope pattern for the m/z 434 ion recorded at 50 V; the 0.5 m/z separation of adjacent peaks is the signature of a doubly-charged ion, in this case caused by oxidation of the ruthenocene moiety.

3.3. Synthesis of [$Ru(\eta^5\text{-}C_5H_5)(CH_3CN)(dppr)][PF_6]\cdot C_6H_{14}$ (**2**) from [$RuCl(\eta^5\text{-}C_5H_5)(dppr)$] (**1**) and NH_4PF_6 in refluxing acetonitrile

A solution of NH_4PF_6 (0.07 g, 0.43 mmol) in dry acetonitrile (40 ml) was added to [$RuCl(\eta^5\text{-}C_5H_5)(dppr)$] (0.20 g, 0.250 mmol) in a Schlenk tube equipped with a reflux condenser topped with a nitrogen bypass. The solution was refluxed for 4 h. After evaporation under vacuum, the residue was extracted with CH_2Cl_2 (5 ml). The extract was filtered through Celite to remove excess NH_4PF_6 and evaporated under reduced pressure. This residue was recrystallized from CH_3CN – hexane (1:4) to give a yellow solid. Yield: 0.18 g, 76%. Anal. Calc. for $C_{47}H_{50}F_6NP_3Ru_2$: C, 54.4; H, 4.9; F, 11.0; N, 1.4; P, 9.0; Ru, 19.5%. Found: C, 54.0; H, 4.00; F, 9.4; N, 1.2; P, 9.6; Ru, 17.1%. δ_H ($CDCl_3$): 2.22 (s, CH_3, 3H); 4.31 (s, Cp, 5H); 4.65 (m, C_5H_4, 2H); 4.72 (m, C_5H_4, 2H); 4.74 (m, C_5H_4, 2H); 4.83 (m, C_5H_4, 2H); 7.26 – 7.54 (m, C_6H_5, 20H) ppm. δ_P: – 144.2 (septet, $J(PF) = 712.1$ Hz); 43.4 (s) ppm.

3.4. Synthesis of [$Ru(\eta^5\text{-}C_5H_5)(CO)(dppr)]Cl$ (**3a**) from [$RuCl(\eta^5\text{-}C_5H_5)(dppr)$] (**1**) and carbon monoxide at 60°C

CO was bubbled into a solution of [$RuCl(\eta^5\text{-}C_5H_5)(dppr)$] (0.02 g, 0.02 mmol) in absolute alcohol (10 ml) at 60°C for 2 h. The reaction mixture was filtered into a Schlenk tube at 0°C, and the solution evaporated to dryness under reduced pressure to give a light-yellow solid (**3a**). ν_{max}: 1968s (CO), 3385s (br), 3050s, 1624w, 1479m, 1433m, 1157m, 1090m, 823w cm^{-1} (CH_2Cl_2). δ_H ($CDCl_3$): 4.83 (s, C_5H_4, 2H); 4.86 (m, C_5H_4, 2H); 4.88 (s, Cp, 5H); 5.10 (m, C_5H_4, 4H); 7.26 – 7.61 (m, C_6H_5, 20H) ppm. δ_P: 48.9 (s) ppm.

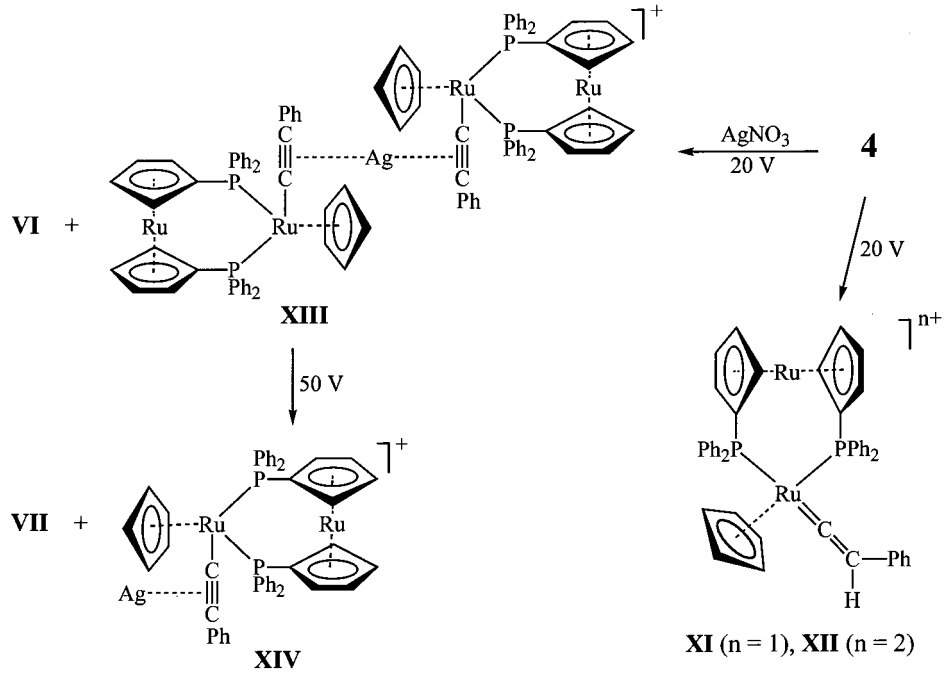

Scheme 4. ESMS fragmentation pattern of [Ru(C=CHPh)(Cp)dppr)]PF_6, **4**, and its addition to $AgNO_3$.

3.5. Synthesis of [Ru(η^5-C_5H_5)(CO)(dppr)][PF_6] (**3b**) from [Ru(η^5-C_5H_5)(CH_3CN)(dppr)][PF_6] (**2**) and carbon monoxide at r.t.

CO was bubbled into a solution of [Ru(η^5-C_5H_5)(CH_3CN)(dppr)][PF_6] (0.02 g, 0.02 mmol) in absolute alcohol (10 ml) at r.t. for 15 min. The light-yellow solid of **3b**·H_2O (yield 86%; m.p. 164–166°C) was isolated similarly to **3a**. Anal. Calc. for $C_{40}H_{35}F_6OP_3Ru_2$: C, 50.2; H, 3.7; F, 11.9; P, 9.7; Ru, 21.1%. Found: C, 49.9; H, 4.1; F, 7.3; P, 9.3; Ru, 15.5%. ν_{max}: 1968s (CO), 831vs (b) (PF_6), 1429m, 1094m cm^{-1} (KBr). δ_H ($CDCl_3$): 4.82 (s, Cp, 5H); 4.82 (m, C_5H_4, 2H); 4.84 (m, C_5H_4, 2H); 5.08 (m, C_5H_4, 4H); 7.26 – 7.57 (m, C_6H_5, 20H) ppm. δ_P: – 144.2 (septet, J(PF) = 712.5 Hz); 48.7 (s) ppm.

3.6. Synthesis of [Ru(C=CHPh)(η^5-C_5H_5)(dppr)][PF_6] · C_6H_{14} (**4**) from [Ru(η^5-C_5H_5)(CH_3CN)(dppr)][PF_6] (**2**)

Excess phenylacetylene was added to [Ru(η^5-C_5H_5)(CH_3CN)(dppr)][PF_6] (0.02 g, 0.02 mmol) in CH_2Cl_2 (10 ml) at r.t. under nitrogen. The solution turned from chrome-yellow to deep red after a few seconds of stirring. It was evaporated to dryness under reduced pressure and the crude solid was recrystallized from CH_2Cl_2–hexane (1:3) to give the reddish–pink product (Yield: 0.02 g, 98%; m.p. 229–232°C). Anal. Calc. for $C_{53}H_{53}F_6P_3Ru_2$: requires C, 57.9; H, 4.9; F, 10.4; P, 8.5; Ru, 18.4%. Found: C, 57.7; H, 4.5; F, 10.6; P, 8.1; Ru, 14.4%. ν_{max}: 1699s (C=C), 1645s (C=C), 838m (br) (PF_6), 1436m, 1080w cm^{-1} (KBr). δ_H ($CDCl_3$): 4.86 (m, C_5H_4, 2H); 4.96 (m, C_5H_4, 2H); 5.06 (m, C_5H_4, 2H); 5.08 (m, C_5H_4, 2H); 5.23 (s, Cp, 5H); 5.64 (t, CH, 1H, J(HP) = 1.9 Hz); 6.84 – 7.50 (m, C_6H_5, 25H) ppm. δ_P: – 144.2 (septet), 50.0 (s) ppm. δ_C: 74.65 (s, γ-C_5H_4); 74.95 (s, γ-C_5H_4); 77.7 (t, β-C_5H_4, J(CP) = 5.7 Hz); 78.5 (t, β-C_5H_4, J(CP) = 4.6 Hz); 88.5 (m, α-C_5H_4); 94.13 (s, Cp); 119.58 (s, =CHPh); 126.78 – 137.85 (m, C_6H_5); 354.00 (t, Ru=C) ppm.

3.7. Electrospray mass spectrometry

Spectra were recorded in positive-ion mode using a VG Platform II instrument employing nitrogen as both the drying and nebulizing gas. The negative-ion spectrum of complex **4** was also recorded, to confirm the presence of the PF_6^- anion. Spectra were an average of ten to 12 scans. A range of cone voltages, from 5 to 50 V were typically used for each sample, to investigate fragmentation pathways. The analyte solution, of approximate concentration 0.1 mM, was delivered to the mass spectrometer source using a Spectra System P1000 HPLC pump, at a flow rate of 0.01 ml min^{-1}. Spectra of dppr were recorded in MeCN solution, to which a small quantity of aqueous $AgNO_3$ solution had been added to generate in situ dppr–Ag^+ complexes. Complexes **2** and **3b** were recorded in 1:1 MeCN–H_2O

solution, while the ESMS sample of complex **4** was prepared by dissolving a small crystal of the complex in a drop of CH_2Cl_2, followed by dilution to 1 ml with MeOH. Pure methanol was used as the mobile phase solvent for this complex. Assignment of major ions was aided by a comparison of the experimental and calculated isotope distribution patterns, the latter obtained using the Isotope program [33].

3.8. X-ray crystallography

Single crystals of $[Ru(\eta^5\text{-}C_5H_5)(CO)(dppr)][PF_6]$, **3b**, were grown by a diffusion method with *n*-hexane layered on a concentrated solution of the complex in CH_2Cl_2 at r.t. Good crystals could also be obtained by a similar method using Et_2O on a concentrated solution of the complex in CH_2Cl_2. A well-formed colorless crystal ($0.16 \times 0.18 \times 0.20$ mm^3) was mounted inside a thin-walled Lindemann glass capillary under an atmosphere of nitrogen. Preliminary characterization and intensity data collection was performed on a Rigaku AFC7R diffractometer at r.t. using graphite-monochromatized Mo–K_α radiation ($\lambda = 0.71073$ Å) powered at 50 kV and 90 mA. Intensity data were collected using ω scans of width $(0.68 + 0.35 \tan\theta)°$ in θ at a rate of 8.0–32.0° min^{-1}. Data for the structure were corrected for Lorentz-polarization factors. An empirical absorption correction based on a series of ψ-scans was applied to the data. A total of 10781 unique reflections, of which 4113, with $|F_o| > 6\sigma|F_o|$ were treated as observed reflections, *n*, and having 465 number of variables, *p*. Atomic coordinates data for $[Ru(\eta^5\text{-}C_5H_5)(CO)(dppr)][PF_6]$, **3b** are listed in Table 4.

The structure was solved with the Patterson superposition method, and refinement was carried out by full-matrix least-squares using the SHELXTL package on a IBM compatible PC computer [34]. All hydrogen atoms were fixed as isotropic ellipsoids in idealized positions in the final cycles of least-squares refinement. The non-hydrogen atoms were allowed anisotropic motion. Refinement on *F* gave the *R* values shown in Table 1 with the weighting scheme $w^{-1} = [\sigma^2|F_o| + 0.0025|F_o|^2]$ and maximum and minimum heights in the final difference map of $+0.75$ and -0.59 e Å^{-3}.

4. Supplementary material available

Lists of thermal parameters and of observed and calculated structure factors for $[Ru(\eta^5\text{-}C_5H_5)(CO)(dppr)][PF_6]$, **3b** are available from the authors upon request.

Table 4
Atomic coordinates of $[Ru(\eta^5\text{-}C_5H_5)(CO)(dppr)][PF_6]$, **3b**; ($\times 10^5$ for Ru atoms, and $\times 10^4$ for others) and equivalent isotropic temperature factors (Å$^2 \times 10^4$ for Ru; Å$^2 \times 10^3$ for others)

Atom	*x*	*y*	*z*	U_{eq}[a]
Ru(1)	20321(7)	6246(4)	17110(3)	503(2)
Ru(2)	−4353(7)	14596(4)	32758(3)	519(2)
C(1)	1311(14)	323(6)	609(5)	81(5)
C(2)	2642(12)	84(7)	768(6)	88(5)
C(3)	2666(11)	−386(6)	1317(6)	81(4)
C(4)	1317(12)	−454(6)	1473(6)	79(4)
C(5)	517(12)	−19(6)	1047(5)	79(4)
C(6)	−648(10)	378(5)	3073(5)	63(3)
C(7)	−1521(11)	552(6)	3580(6)	76(4)
C(8)	−757(12)	806(6)	4175(6)	79(4)
C(9)	616(10)	799(5)	4072(4)	64(3)
C(10)	690(9)	536(4)	3373(4)	52(3)
C(11)	676(9)	2321(4)	2982(4)	54(3)
C(12)	−218(10)	2570(5)	3426(5)	68(4)
C(13)	−1517(10)	2439(5)	3101(40	64(3)
C(14)	−1404(9)	2103(5)	2446(4)	59(3)
C(15)	−30(9)	2038(5)	2373(4)	54(3)
C(16)	3632(11)	1102(5)	1799(4)	66(4)
O(1)	4673(8)	1368(4)	1798(4)	95(3)
P(1)	728(2)	1637(1)	1635(1)	49(1)
C(17)	2424(11)	2266(6)	745(5)	76(4)
C(18)	2966(11)	2819(8)	418(6)	88(5)
C(19)	2757(13)	3463(8)	648(7)	93(5)
C(20)	2000(14)	3577(6)	1181(6)	91(5)
C(21)	1407(11)	3037(5)	1496(5)	68(4)
C(22)	1586(9)	2376(5)	1287(4)	59(3)
C(23)	−949(11)	1962(6)	380(4)	70(4)
C(24)	−2099(13)	1919(7)	−77(5)	88(5)
C(25)	−3146(13)	1499(8)	76(6)	98(5)
C(26)	−3015(10)	1103(6)	679(6)	76(4)
C(27)	−1821(9)	1142(5)	1139(5)	65(3)
C(28)	−788(10)	1561(5)	1006(4)	58(3)
P(2)	2199(2)	420(1)	2929(1)	47(1)
C(29)	3886(11)	−723(5)	2963(5)	71(4)
C(30)	4302(13)	−1385(6)	3187(6)	85(5)
C(31)	3538(15)	−1770(6)	3582(6)	88(5)
C(32)	2310(14)	−1528(6)	3751(6)	88(5)
C(33)	1890(10)	−873(5)	3542(5)	69(4)
C(34)	2685(9)	−463(5)	3154(4)	56(3)
C(35)	4181(10)	579(5)	4078(5)	69(4)
C(36)	5196(11)	920(6)	4479(5)	78(4)
C(37)	5540(10)	1574(6)	4320(5)	71(4)
C(38)	4881(10)	1884(15)	3761(5)	68(4)
C(39)	3874(9)	1541(5)	3340(4)	54(3)
C(40)	3498(9)	887(5)	3490(4)	51(3)
P(3)	3182(3)	3972(2)	3589(2)	87(1)
F(1)	2760(15)	3353(5)	4019(5)	208(7)
F(2)	3645(15)	4558(6)	3117(7)	215(7)
F(3)	4636(11)	3673(8)	3536(10)	119(5)
F(4)	3932(24)	4291(10)	4281(7)	146(7)
F(5)	1991(30)	4451(17)	3741(22)	264(17)
F(6)	2514(37)	3669(16)	2882(10)	243(14)
F(3′)	4605(21)	3934(21)	4017(20)	270(16)
F(4′)	2705(30)	4507(10)	4119(12)	164(8)
F(5′)	1724(11)	4003(8)	3159(8)	108(5)
F(6′)	3336(20)	3401(8)	3006(8)	125(6)

[a] U_{eq} defined as one third of the trace of the orthogonalized U_{ij} tensor.

Acknowledgements

The authors acknowledge the National University of Singapore (NUS) and Hong Kong Research Grants Council (Ref. CUHK 311/94P) for financial support. W.H. thanks the University of Waikato and the New Zealand Lottery Grants Board for funding of the mass spectrometer. Experimental assistance from A.S.W. Fong and stenographic help from Y.P. Leong are appreciated.

References

[1] (a) L.S. Hegedus, in: M. Schlosser (Ed.), Organometallics in Synthesis—A Manual, Wiley, Chichester, 1994, p. 383. (b) G.W. Parshall, S.D. Ittel, Homogeneous Catalysis: The Applications and Chemistry of Catalysis by Soluble Transition Metal Complexes, 2nd ed., Wiley, New York, 1992.
[2] (a) J. Louie, M.S. Driver, B.C. Hamann, J.F. Hartwig, J. Org. Chem. 62 (1997) 1268. (b) T. Ishiyama, M. Mori, A. Suzuki, N. Miyaura, J. Organomet. Chem. 525 (1996) 225.
[3] M.S. Driver, J.F. Hartwig, J. Am. Chem. Soc. 118 (1996) 7217.
[4] S. Li, B. Wei, P.M.N. Low, H.K. Lee, T.S.A. Hor, T.C.W. Mak, J. Chem. Soc. Dalton Trans. (1997) 1289.
[5] B. Wei, S. Li, H.K. Lee, T.S.A. Hor, J. Organomet. Chem. 527 (1997) 133.
[6] A.P. Snyder (Ed.), Biochemical and Biotechnological Applications of Electrospray Ionisation Mass Spectrometry, ACS, Washington DC, 1995.
[7] For examples see: (a) W. Henderson, J.S. McIndoe, B.K. Nicholson, P.J. Dyson, Chem. Commun. 10 (1996) 1183. (b) M.B. Dinger, W. Henderson, B.K. Nicholson, A.L. Wilkins, J. Organomet. Chem. 526 (1996) 303. (c) R. Colton, A. D'Agostino, J.C. Traeger, Mass Spectrom. Rev. 14 (1995) 79. (d) R.T. Aplin, H. Doucet, M.W. Hooper, J.M. Brown, Chem. Commun. (1997) 2097. (e) H. Hori, F.P.A. Johnson, K. Koike, K. Takeuchi, T. Ibusuki, O. Ishitani, J. Chem. Soc. Dalton Trans. (1997) 1019.
[8] (a) T. Lover, G.A. Bowmaker, W. Henderson, R.P. Cooney, Chem. Commun. 5 (1996) 683. (b) K.J. Fisher, W. Henderson, I.G . Dance, G.D. Willett, J. Chem. Soc. Dalton Trans. (1996) 4109.
[9] (a) G.S. Ashby, M.I. Bruce, I.B. Tomkins, R.C. Wallis, Aust. J. Chem. 32 (1979) 1003. (b) M.I. Bruce, I.R. Butler, W.R. Cullen, G.A. Koutsantonis, M.R. Snow, E.T. Tiekink, Aust. J. Chem. 41 (1988) 963.
[10] (a) G. Consiglio, F. Morandini, Chem. Rev. 87 (1987) 761. (b) G. Consiglio, F. Morandini, G.F. Ciani, A. Sironi, Organometallics 5 (1986) 1976.
[11] (a) C. Masters, Homogeneous Transition-metal Catalysis: A Gentle Art, Chapman and Hall, London, 1981, p. 52. (b) B.R. James, L.D. Markham, D.K. Wang, J. Chem. Soc. Chem. Commun. (1974) 439. (c) J. Tsuji, H. Suzuki, Chem. Lett. (1977) 1083.
[12] (a) R. Noyori, H. Takaya, Acc. Chem. Res. 23 (1990) 345. (b) H. Takaya, T. Ohta, R. Noyori, K. Mashima, Pure Appl. Chem. 62 (1990) 1135. (c) K. Mashima, Y. Matsumura, K. Kusano, H. Kumobayashi, N. Sayo, Y. Hori, T. Ishizaki, S. Akutagawa, H. Takaya, J. Chem. Soc. Chem. Commun. (1991) 609. (d) Monsanto, World Patent WO9,015,790A, 1991.
[13] J.M. Brown, P.J. Guiry, Inorg. Chim. Acta 220 (1994) 249.
[14] T. Blackmore, M.I. Bruce, F.G.A. Stone, J. Chem. Soc. (A) (1971) 2376.
[15] M.I. Bruce, F.S. Wong, B.W. Skelton, A.H. White, J. Chem. Soc. Dalton Trans. (1981) 1398.
[16] S. Onaka, T. Moriya, S. Takagi, A. Mizuno, H. Furuta, Bull. Chem. Soc. Jpn. 65 (1992) 1415.
[17] (a) M.I. Bruce, R.C. Wallis, Aust. J. Chem. 32 (1979) 1471. (b) M. Sato, M. Sekino, J. Organomet. Chem. 444 (1996) 185.
[18] P.T. Czech, X.G. Xe, R.F. Fenske, Organometallics 9 (1990) 2016.
[19] R.M. Bullock, J. Chem. Soc. Chem. Commun. (1989) 165.
[20] M. Sato, M. Asa, J. Organomet. Chem. 508 (1996) 121.
[21] (a) M.I. Bruce, Chem. Rev. 91 (1991) 197. (b) M.I. Bruce, Pure Appl. Chem. 62 (1990) 1021. (c) I. de los Ríos, M.J. Tenorio, M.C. Puerta, P. Valerga, J. Am. Chem. Soc. 119 (1997) 6529. (d) R. Le Lagadec, E. Roman, L. Toupet, U. Müller, P.H. Dixneuf, Organometallics 13 (1994) 5030. (e) S.G. Davies, J.P. McNally, A.J. Smallridge, Adv. Organomet. Chem. 30 (1990) 1. (f) J. Silvestre, R. Hoffmann, Helv. Chim. Acta 68 (1985) 1461.
[22] (a) F.J.G. Alonson, A. Höhn, J. Wolf, H. Otto, H. Werner, Angew. Chem. Int. Ed. Engl. 24 (1985) 406. (b) K.R. Birdwhistell, T.L. Tonker, J.L. Templeton, J. Am. Chem. Soc. 107 (1985) 4474.
[23] C. Bianchini, M. Peruzzini, A. Vacca, F. Zanobini, Organometallics 10 (1991) 3697.
[24] Y. Wakatsuki, N. Koga, H. Werner, K. Morokuma, J. Am. Chem. Soc. 119 (1997) 360.
[25] (a) B.M. Trost, R.J. Kulawiec, J. Am. Chem. Soc. 114 (1992) 5579. (b) Y. Nishibayashi, I. Takei, M. Hidai, Organometallics 16 (1997) 3091.
[26] W. Henderson, G.M. Olsen, Polyhedron 17 (1998) 577.
[27] W. Henderson, M. Sabat, Polyhedron 16 (1997) 1663.
[28] M.I. Bruce, M. Ke, P.J. Low, Chem. Commun. (1996) 2405.
[29] W. Henderson, B.M. Nicholson, J. Chem. Soc. Chem. Commun. (1995) 2531.
[30] (a) M. Oliván, O. Eisenstein, K.G. Caulton, Organometallics 16 (1997) 2227. (b) M. Oliván, E. Clot, O. Eisenstein, K.G. Caulton, Organometallics 17 (1998) 3091.
[31] (a) D.F. Shriver, M.A. Drezdzon, The Manipulation of Air-Sensitive Compounds, 2nd ed., Wiley-Interscience, New York, 1986. (b) J.P. McNally, V.S. Leong, N.J. Cooper, in: A.L. Wayda, M.Y. Darensbourg (Eds.), Experimental Organometallic Chemistry—A Practicum in Synthesis and Characterisation, ACS Symposium Series 357, ACS, Washington DC, 1987.
[32] A.J. Gordon, R.A. Ford, The Chemist's Companion: A Handbook of Practical Data, Techniques and References, Wiley-Interscience, New York, 1972.
[33] L.J. Arnold, J. Chem. Educ. 69 (1992) 811.
[34] (a) SHELXTL Version 5 Reference Manual, Siemens Energy&Automation, Madison, WI, 1996. (b) G.M. Sheldrick, in: H.D. Flack, L. Párkányi, K. Simon (Eds.), Crystallographic Computing 6: A Window in Modern Crystallography, Oxford University Press, New York, 1993, pp. 100–122.